Histol Histopathol (2013) 28: 327-335
DOI: 10.14670/HH-28.327

http://www.hh.um.es

Histology and Histopathology
Cellular and Molecular Biology

Histological examination on osteoblastic activities in the alveolar bone of transgenic mice with induced ablation of osteocytes

Minqi Li[1,2,3], Tomoka Hasegawa[3], Hiromi Hogo[3], Sawako Tatsumi[4], Zhusheng Liu[3], Ying Guo[3], Muneteru Sasaki[3], Chihiro Tabata[3], Tsuneyuki Yamamoto[3], Kyoji Ikeda[4] and Norio Amizuka[3]

[1]Department of Bone Metabolism, School of Stomatology, Shandong University, [2]Shandong Provincial Key Laboratory of Oral Biomedicine, Jinan, China [3]Department of Developmental Biology of Hard Tissue, Graduate School of Dental Medicine, Hokkaido University, Sapporo, Japan and [4]Department of Bone and Joint Disease, National Center for Geriatrics and Gerontology, Obu, Aichi, Japan

Summary. The purpose of this study was to examine histological alterations on osteoblasts from the alveolar bone of transgenic mice with targeted ablation of osteoctyes. Eighteen weeks-old transgenic mice based on the diphtheria toxin (DT) receptor-mediated cell knockout (TRECK) system were used in these experiments. Mice were injected intraperitoneally with 50 μg/kg of DT in PBS, or only PBS as control. Two weeks after injections, mice were subjected to transcardiac perfusion with 4% paraformaldehyde in 0.1M phosphate buffer (pH 7.4), and the available alveolar bone was removed for histochemical analyses. Approximately 75% of osteocytes from alveolar bones became apoptotic after DT administration, and most osteocytic lacunae became empty. Osteoblastic numbers and alkaline phosphatase (ALP) activity were markedly reduced at the endosteum of alveolar bone after DT administration compared with the control. Osteoblastic ALP activity in the periodontal ligament region, on the other hand, hardly showed any differences between the two groups even though numbers were reduced in the experiment group. Silver impregnation showed a difference in the distribution of bone canaliculi between the portions near the endosteum and the periodontal ligament: the former appeared regularly arranged in contrast to the latter's irregular distribution. Under transmission electron microscopy (TEM), the osteoblasts in the periodontal ligament showed direct contact with the Sharpey's fibers. Thus, osteoblastic activity was affected by osteocyte ablation in general, but osteoblasts in contact with the periodontal ligament were less affected than endosteal osteoblasts.

Key words: Alveolar bone, Osteocyte, Osteoblast, Bone canalicular, Sharpey's fiber

Offprint requests to: Minqi Li, DDS, PhD, Department of Bone Metabolism, School of Stomatology, Shandong University, Shandong Provincial Key Laboratory of Oral Biomedicine, Wenhua West Road 44-1, Jinan 250012, China. e-mail: li_min_qi@hotmail.com

Introduction

Osteocytes are the most abundant cells in bone, forming a network among themselves and with osteoblasts located on the bone matrix surface via long cytoplasmic extensions that occupy tiny canals called canaliculi, which are used for exchange of nutrients and cellular waste (Doty, 1981; Ejiri and Ozawa, 1982). Cowin reported that the bone fluid flow through the canaliculi not only exchanged nutrients and waste but also exerted pressure on the cell processes, which is large enough for the cells to sense (Cowin, 2002). Osteocytes communicate to other cells through the bone canaliculi network, playing pivotal roles in the activation and function of osteoblasts (Burger and Klein-Nulend, 1999). Marotti et al. demonstrated that osteocytes might modulate osteoblastic activity and recruit osteoblasts that differentiate into osteocytes through inhibitory signals transmitted via gap junctions (Marotti et al., 1992). In addition, actin fibers existing in bone canaliculi have been shown to participate in process shrinkage, material transport and intracellular signaling mechanisms (Palumbo et al., 1990).

Diphtheria toxin is an exotoxin secreted by *Corynebacterium diphtheriae*, the bacterium that causes diphtheria. Because murine cells are naturally resistant

to diphtheria toxin, Saito et al. established a transgenic mouse model based on the diphtheria toxin receptor-mediated cell knockout (TRECK) system (Saito et al., 2001). In short, the diphtheria toxin receptor is expressed in transgenic mice using a specific promoter; then, the diphtheria toxin is injected, causing the targeted cells to die. We have previously used the dentin matrix protein-1 (DMP-1) promoter, which was originally identified in dentin, to direct the expression of the diphtheria toxin receptor specifically in osteocytes, and injected diphtheria toxin to induce osteocyte ablation (Tatsumi et al., 2007).

In the alveolar region, periodontal ligament and alveolar bone keep close anatomical contact. Alveolar bone forms the tooth socket surrounding the roots of teeth, and periodontal ligament exercises the function of attaching teeth to the alveolar bone, helping them to withstand the naturally substantial compressive stresses. Anatomically, alveolar bone is divided into two parts: the outer intrinsic alveolar bone and inner support alveolar bone. The intrinsic alveolar bone is referred to as bundle bone containing the extrinsic collagen fiber bundles of the periodontal ligament, while the support alveolar bone is composed of external cortical plates and inner cancellous bone with bone marrow. The periodontal ligament's collagen fiber bundles are called Sharpey's fibers. Following these anatomical division, osteoblasts located on the surface of the intrinsic alveolar bone directly contact the Sharpey's fibers, whereas the osteoblasts on the endosteal side of support alveolar bone marrow do not (Kapur and Russell, 1978; Kuroiwa et al., 1994).

To date, there have been few reports focusing on the morphological relationship among osteocytes, osteoblasts and collagen fibers in the region of alveolar bone. Thus, we set out to collect some histological evidence of osteoblastic activities influenced by osteocytes and Sharpey's fibers in the alveolar bone using the previously mentioned transgenic mice model with DT administration. We found contrasting situations between osteoblasts on the surface of intrinsic alveolar bone and on the endosteum of support alveolar bone after osteocytes were ablated. In addition to routine histochemical techniques, silver staining was performed to observe the specific situation of bone canaliculi arrangement within the alveolar bone.

Materials and methods

Animal and tissue preparation

All animal experiments were conducted according to the Guidelines for Animal Experimentation of Hokkaido University. Part of the alveolar bone of transgenic mice that were used in a previous study (Tatsumi et al., 2007) was used in the present study. Eighteen weeks-old transgenic mice were injected intraperitoneally with diphtheria toxin in PBS (50 μg/kg of body weight) or PBS only as control. Two weeks after injection, mice were subjected to transcardiac perfusion with 4% paraformaldehyde in a 0.1M phosphate buffer (pH 7.4) after anesthesia with an intraperitoneal injection of chloral hydrate. Mandibles were removed and immersed in the same fixative for other 12h prior to decalcification with 10% EDTA-2Na (ethylenediamine tetraacetic acid disodium salt) solution for 3 weeks at 4°C. After that, specimens were dehydrated with ethanol solutions in ascending concentrations prior to paraffin embedding. The first molar and its interradicular septum were considered the region of interest in this experiment.

The specimens for transmission electron microscopy (TEM) were decalcified with 5% EDTA-2Na solution and post-fixed with a mixture of 1% OsO_4 and 1.5% potassium ferrocyanide in 0.1M cacodylate buffer (pH 7.4) for 4 h at 4°C. They were, then, dehydrated with ascending concentrations of acetone, and embedded in epoxy resin. (Epon 812; Taab Laboratories, UK). Ultrathin sections were made by a microtome (Sorvall MT-5000; Ivan Sorvall, Inc., Norwalk, CT) and then stained with uranyl acetate, lead citrate, and tannic acid prior to TEM observation (H-7100; Hitachi Co. Ltd, Tokyo, Japan) at 80 KV.

Immunohistochemistry for RANKL and double staining for ALPase and TRAPase

After xylene treatment, dewaxed paraffin sections were pretreated with 0.3% hydrogen peroxide for 30 min, and then with 1% bovine serum albumin (BSA; Seologicals Proteinss Inc. Kankakee, IL, USA) in PBS (1% BSA-PBS) for 20 min. The treated sections were incubated with the primary antibody of rabbit serum to tissue nonspecific alkaline phosphatase (ALPase) (Oda et al., 1999), rat anti-RANKL (receptor activator of nuclear actor kappa-B ligand, Oriental Yeast Co., LTD., Tokyo, Japan) at a dilution of 1:150 with 1% BSA-PBS for 2 h at room temperature. They were then immersed in horseradish peroxidase (HRP)-conjugated secondary antibodies (Chemicon International Inc., Temecula, CA, USA) at a dilution of 1:100 for 1 h at room temperature. Visualization was achieved with the aid of a diaminobenzidine (DAB) substrate. After satisfactory immunostaining, the sections treated with ALPase antibody were rinsed with PBS and submerged in a mixture of 3.0 mg of naphthol AS-BI phosphate, 18 mg of red violet LB salt, and 100 mM L(+) tartaric acid (0.36g) diluted in 30 mL of 0.1M sodium acetate buffer (PH 5.0) for 15 min at 37ºC. Staining results were assessed under light microscopy, and all sections were faintly counterstained with methyl green.

Simple silver staining and double silver staining and ALPase

Dewaxed paraffin sections were pretreated in 1% albumosesilver solution with pieces of copper for 36 h at 37°C before reaction with a mixture solution containing 0.3 g hydroquinone, 0.3 g citric acid and 1 g silver

nitrate and 140 ml distilled water for 2 min at room temperature. Then, these sections were treated with amidol solution made by sulfurous anhydride 5 g, potassium bromide 1 g and amidol 1 g in 200 ml distilled water, 1% chloradric acid solution, 2% oxalic acid dehydrate and 5% sodium thiosulfate solutions, respectively. As for the double staining, ALPase immunostaining was performed after silver staining, as previously described (Ubaidus et al., 2009).

Statistical analysis

ImagePro Plus 6.2 software (Media Cybernetics, Silver Spring, MD) was used for counting the number of vital osteocytes and empty lacunae in the alveolar bone of the DT-treated group and control, and results were statistically analyzed (n=6 per group). In addition, the numbers of ALPase-positive osteoblasts and TRAPase-positive osteoclasts of both groups were also measured, with statistical analysis performed afterwards. All values are presented as means±standard deviation. Differences among the groups were assessed by the Student's t-test, and considered statistically significant at $P<0.05$.

Results

Histology of osteocytes and osteoblasts in the alveolar bone

Two weeks after DT administration, the alveolar bone of transgenic mice showed increased numbers of empty lacunae when compared with the control (Figs. 1B,C). Statistical analysis revealed a significant difference between the groups with regards to the number of empty lacunae (15.17±3.71 in control vs 74.17±3.76 in the DT administration group, $P<0.005$). Approximately 75% of the osteocytes in the alveolar bone underwent cell death and most bone lacunae became empty in the DT-administered group (Fig. 1D). A typical osteoblastic layer could be found on the

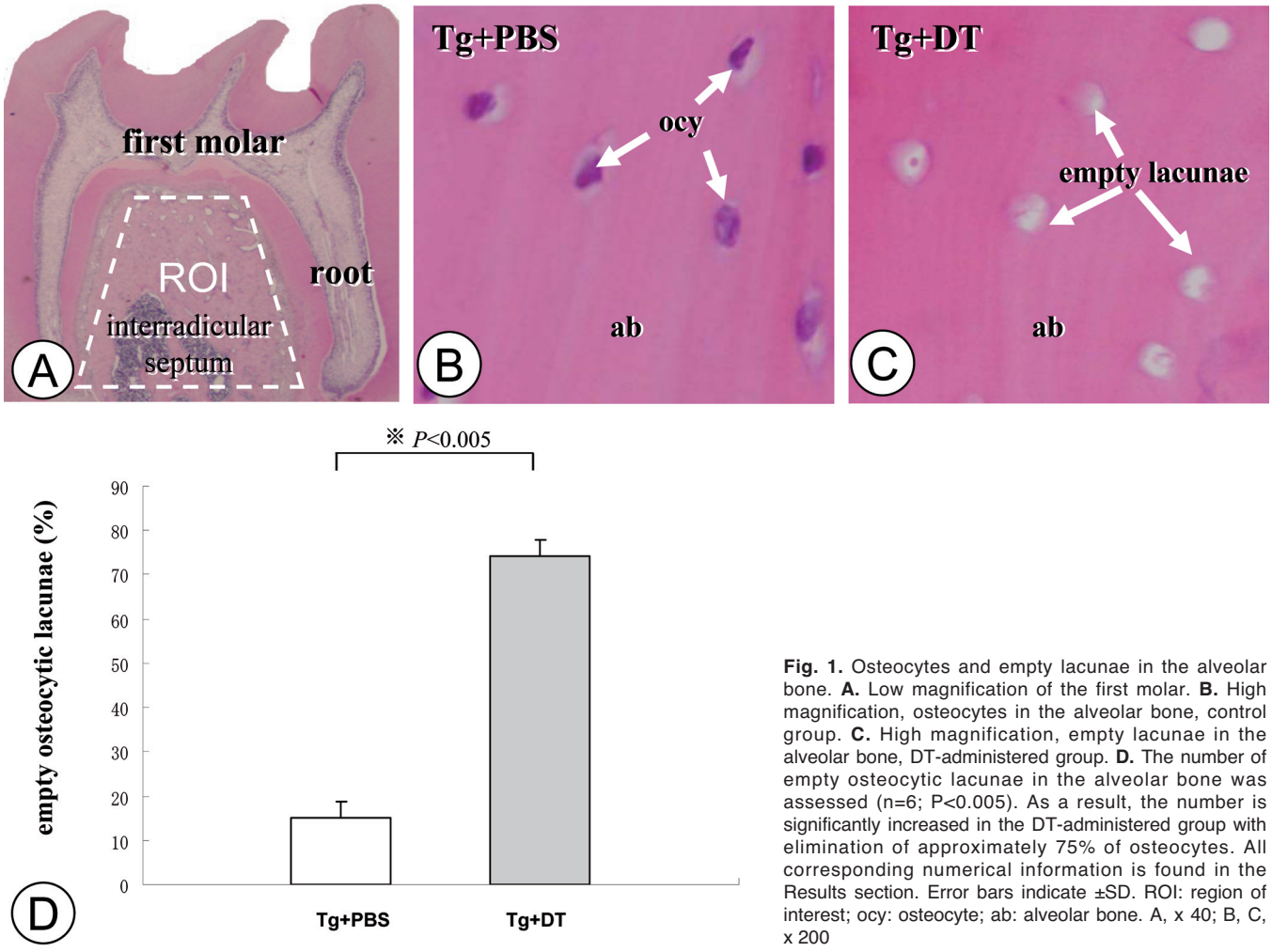

Fig. 1. Osteocytes and empty lacunae in the alveolar bone. **A.** Low magnification of the first molar. **B.** High magnification, osteocytes in the alveolar bone, control group. **C.** High magnification, empty lacunae in the alveolar bone, DT-administered group. **D.** The number of empty osteocytic lacunae in the alveolar bone was assessed (n=6; $P<0.005$). As a result, the number is significantly increased in the DT-administered group with elimination of approximately 75% of osteocytes. All corresponding numerical information is found in the Results section. Error bars indicate ±SD. ROI: region of interest; ocy: osteocyte; ab: alveolar bone. A, x 40; B, C, x 200

endosteal side and on the periodontal ligament region of the alveolar bone of control transgenic mice (Figs. 2B,C); on the other hand, osteoblastic numbers were reduced in the alveolar bone of transgenic mice administered with DT (Figs. 2E,F). Interestingly, osteoblasts could scarcely be found on the endosteal surface of the alveolar bone in DT-administered samples (Fig. 2E).

Immunolocalization of ALPase and bone canaliculi arrangement in the alveolar bone

Bone canaliculi connecting osteocytes among themselves and to osteoblasts on the endosteal surface of the alveolar bone showed a regular arrangement as shown by silver impregnation (Fig. 3A,C); however, bone canaliculi in the area close to the periodontal ligament showed an irregular distribution of the osteocytic network (Fig. 3B,D). Osteoblasts stained intensely for ALPase both on the endosteal and the periodontal ligament surfaces of the control group (Fig. 3A,B). In the DT-administered group, in contrast, osteoblasts located on the endosteal surface were flat bodied with weak ALPase activity (Fig. 3C); while osteoblasts on the periodontal ligament surface stained similarly for ALPase when compared to control, overall cell number in that area was lower in DT-administered samples (Fig. 3D).

Statistical analysis of osteoblastic numbers

The number of ALPase-positive osteoblasts showed a significant difference between the DT-administered group and control in the endosteal (9.17±1.47 in control vs 3.17±0.75 in the DT administration group, $P<0.005$) and the periodontal ligament areas (9.67±1.63 in control vs 6.50±1.87 in the DT administration group, $P<0.05$). In addition, we have identified a significant difference between the endosteal and periodontal ligament areas with regards to the number of ALPase-positive osteoblasts after osteocytes ablation (3.17±0.75 in the endosteal surfaces vs 6.50±1.87 in the periodontal

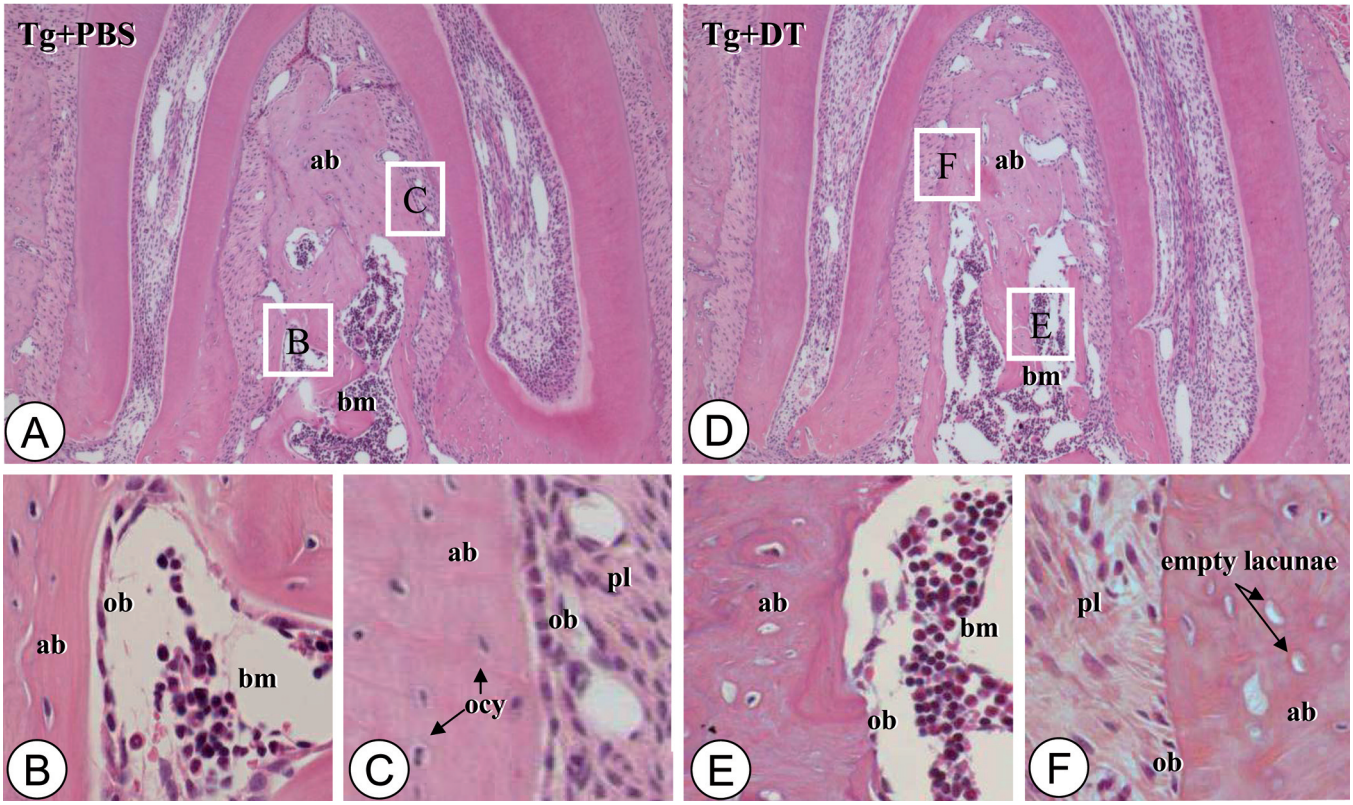

Fig. 2. Histology of osteoblasts. **A, D.** Low magnification of alveolar bone of transgenic mice with PBS injection **(A)** and DT administration **(D)**. **Panels B, C, E and F.** show higher magnifications for endosteal and periodontal ligaments areas in control **(B, C)** and DT-administered mice **(E, F)**, respectively. The alveolar bone of transgenic mice after DT administration showed a larger number of empty lacunae. Moreover, there were fewer osteoblasts at both the endosteal and the periodontal ligament region of the DT-administered alveolar bone. Only few osteoblasts could be found on the endosteal surface of DT-administered alveolar bone **(E)**. bm: bone marrow; ob: osteoblast; pl: periodontal ligament; ab: alveolar bone. A, D, x 40; B, C, E, F, x 100

ligament area, P<0.01).

TRAPase staining for osteoclasts on the endosteal surfaces and statistical analysis of osteoclastic numbers

Osteoclasts existing on the endosteal surfaces of the alveolar bone showed increases in number and in activity after DT administration (Fig. 4A,B). Statistical analysis found a significant difference in osteoclastic numbers between the control and the experiment group (3.00±0.89 vs 9.00±1.41, P<0.005, Fig 4E). RANKL immunolocalization could not be verified in the osteocytes of the alveolar bone (Fig. 4C,D).

TEM imaging for the positional relationship of osteoblasts and collagen fibrils in the periodontal ligament region

Osteoblasts located on the periodontal ligament surface of the alveolar bone contacted with the collagen fibril bundles (Sharpey's fibers), which attached to the alveolar bone at a right angle in the control group (Fig. 5A,B). Moreover, osteoblasts seemed to have maintained their activity, as judged by the cuboidal shape characteristic of active cells. That is to say, intense osteoblastic activity was maintained even after osteocytes were targeted for ablation and which may be due to direct cell-fiber contact.

Discussion

In this study, we investigated osteoblastic activity in different areas of the alveolar bones of a transgenic mice model with targeted ablation of osteocytes (Tatsumi et al., 2007). As shown in Fig. 1D, approximately 75% of the osteocytes were eliminated and large numbers of empty lacunae were observed in the alveolar bone of the experimental group after DT injection. Accordingly, osteoblast number and activity were markedly reduced on the endosteal surfaces of the DT-administered group. On the other hand, a regular arrangement of the bone canaliculi was found in the endosteal portion of the

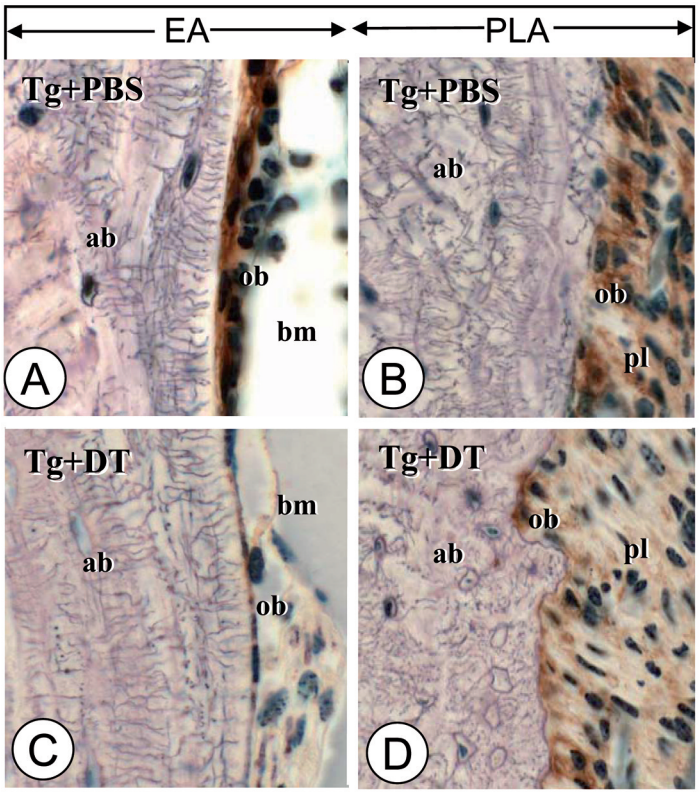

EA: endosteum area; PLA: periodontal ligament area

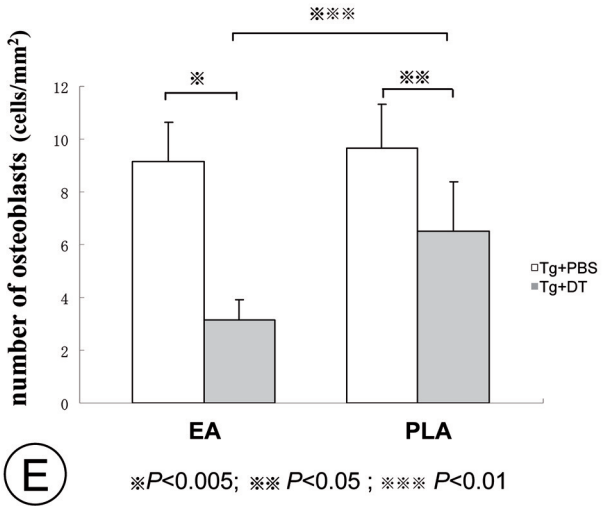

Fig. 3. Double staining for ALPase/silver staining and statistical analysis for ALPase-positive osteoblasts. **A, C.** The endosteal area of the alveolar bone in control and DT-administered samples contained osteoblasts with strong **(A)** and weak **(C)** ALPase staining, respectively. **B, D.** The periodontal ligament region of the alveolar bone showed similar ALPase staining intensities in both groups control **(B)** and DT-administered **(D)**, but fewer osteoblasts were identified in the experimental group. Moreover, note that bone canaliculi were regularly arranged in the portion near the endosteum of the support alveolar bone (**A, C**), while an irregular distribution was seen in the intrinsic alveolar bone close to the periodontal ligament region (**B, D**). **E.** ALPase-positive osteoblasts were counted in the endosteal and periodontal ligaments regions of the alveolar bone for both groups (n=6). Fewer ALPase-positive osteoblasts were seen in both the endosteal and the periodontal ligaments of the DT-administered group (EA: P<0.005, PLA: P<0.05). There was also a significant difference between the endosteal and periodontal ligament areas with regards to the number of ALPase-positive osteoblasts after osteocytes ablation. All corresponding numerical information is found in the Results section. Error bars indicate ±SD. bm: bone marrow; ob: osteoblast; pl: periodontal ligament; ab: alveolar bone; EA: endosteum area; PLA: periodontal ligatment area. A-D, x 150

alveolar bone, as revealed by silver staining (Fig. 3A,C), implying that communication between osteocytes and osteoblasts was preserved in that area. This is consistent with previous studies showing that osteocytes may regulate osteoblastic activities via their canaliculi (Kufahl and Saha, 1989; Marotti et al., 1992; Li et al., 2004; Damian et al., 2007; Adachi et al., 2009). Osteocytes ablation may significantly reduce sclerostin, a canonical Wnt signal inhibitor that binds to LRP-5 and -6 (Ott, 2005; Poole et al., 2005; Semënov et al., 2005; Masuki et al., 2010). With less sclerostin, osteoblastic activity should be enhanced; in our observations, however, osteoblasts appeared flat and stained weakly for ALPase on the endosteal surfaces of DT-administered alveolar bones. Considerations shold be given, therefore, to the existence of other osteocyte-derived factors that regulate osteoblastic activity.

Another interesting finding of this experiment is that numerous osteoclasts were observed on the endosteal surfaces of DT-administered alveolar bones, which induced the formation of wider bone marrow cavities (data not shown). Such finding is inconsistent with a recent report showing that osteoclastic formation is critically dependent on osteocyte-derived RANKL (Nagashima et al., 2011). Because of particularity of alveolar bone, further investigation is necessary to verify this anatomically critical event. It is widely accepted that osteoblasts play an essential role in supporting osteoclast formation and bone-resorbing activity through RANK-RANKL system (Fuller et al., 1998; Takami et al., 1999; Udagawa et al., 1999, 2000). In the present study, however, fewer osteoblasts with reduced ALPase activity were found on the endosteal surface of the alveolar bone, along with an increased number of TRAP-positive osteoclasts. These histological findings support previous notions that osteocytes may regulate osteoclastogenesis and activation via soluble signals (Tan et al., 2007; You et al., 2008) and that apoptotic osteocytes regulate osteoclast precursor recruitment and differentiation (Al-Dujaili et al., 2011). This means that the increase in osteoclastic numbers on the endosteal surfaces of DT-administered alveolar bones may result from targeted osteocytes ablation.

Periodontal osteoblasts play an important role in physiological remodeling and metabolic breakdown of collagen fibrils from the periodontal ligament, unpaired with osteoclastic bone remodeling (Yajima et al., 1999). In the present study, bone canaliculi appeared irregularly arranged close to the periodontal ligament (Fig. 3B,D), in contrast to the situation in the endosteal area. Interestingly, bone canaliculi appeared to contact neither the osteocyte lacunae nor the osteoblasts in the area close to the surface of the alveolar bone. However, osteoblasts in the periodontal ligament of the DT-

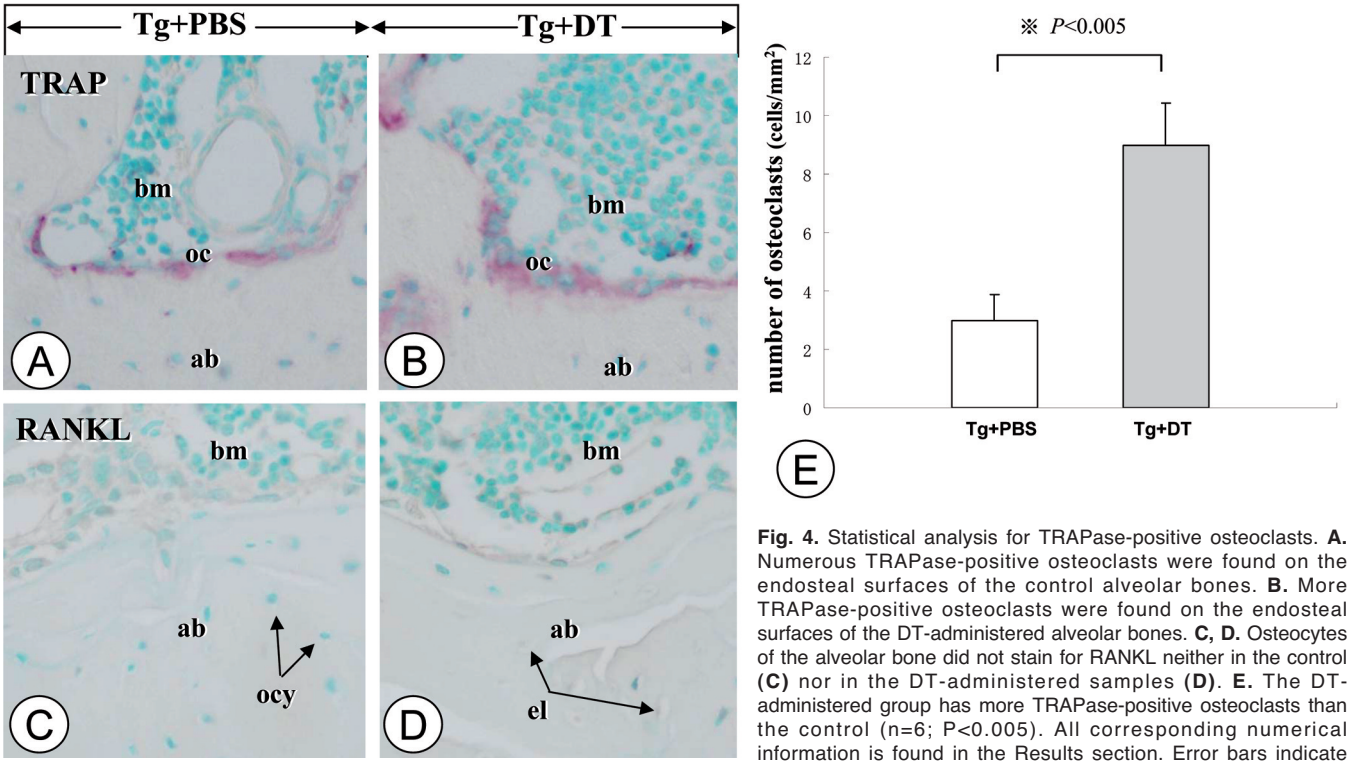

Fig. 4. Statistical analysis for TRAPase-positive osteoclasts. **A.** Numerous TRAPase-positive osteoclasts were found on the endosteal surfaces of the control alveolar bones. **B.** More TRAPase-positive osteoclasts were found on the endosteal surfaces of the DT-administered alveolar bones. **C, D.** Osteocytes of the alveolar bone did not stain for RANKL neither in the control **(C)** nor in the DT-administered samples **(D)**. **E.** The DT-administered group has more TRAPase-positive osteoclasts than the control (n=6; P<0.005). All corresponding numerical information is found in the Results section. Error bars indicate ±SD. bm: bone marrow; oc: osteoclast; ab: alveolar bone; ocy: osteocyte; el: empty lacunae. A, B, x 150

administered group still featured strong ALP staining, similar to that of the control group (Fig. 3B,D). We speculate that osteoblastic activity may be maintained by factors other than communication with osteocytes via canaliculi in the periodontal ligament region, such as mechanical loading stimulation.

Collagen fibril bundles, or Sharpey's fibers, are abundantly distributed in the area of alveolar bone and periodontal ligament as shown in Fig. 5. Under TEM, osteoblasts appear in direct contact with the Sharpey's fibers, which come from the periodontal membrane attaching to the alveolar bone at a right angle. Also, osteoblasts in the experimental group show round or elliptical shapes and similar ALP activity to that of their control counterparts (Fig. 3B,D). Previous studies have reported that mechanical loading stimulates osteoblast precursor cells to rapidly respond by entering a differentiation pathway through effective expression of type I collagen and alkaline phosphatase genes (Pavlin et al., 2000, 2001). Mastication also produces changes in Sharpey's fibers that contact osteoblasts (Martinez and Johnson, 1987). In addition, several researchers have reported that ascorbic acid has a relationship with osteoblastic differentiation in the periodontal ligament (Shiga et al., 2003; Ishikawa et al., 2004; Mimori et al., 2007). Hence, the preservation of osteoblastic activity in the periodontal ligament region even after osteocytes ablation may be attributed to physiological mechanical loading via direct fiber-to-cell contact (Fig. 5C).

In summary, osteoblastic activities were not only affected by the targeted ablation of osteocytes, but were also influenced by direct fiber-to-cell contact in our

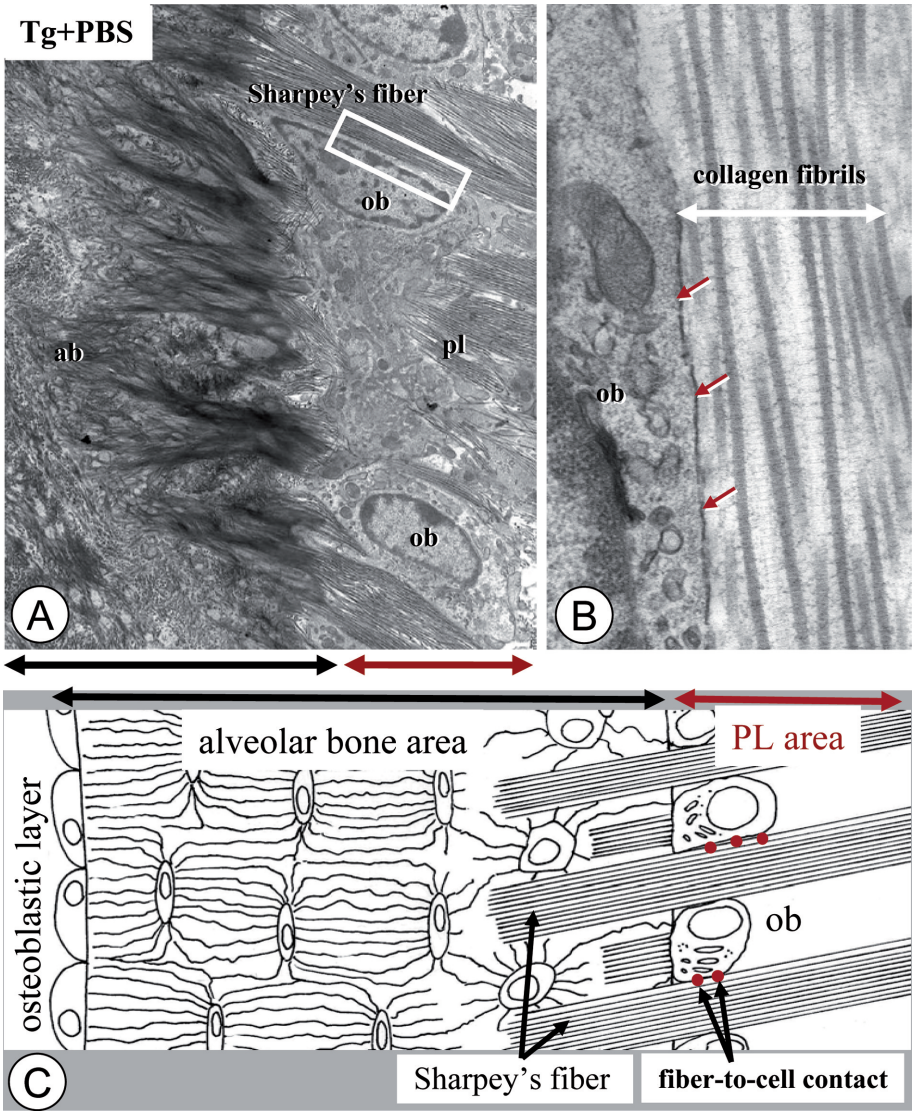

Fig. 5. Electron micrographs of Sharpey's fibers and osteoblasts at the periodontal ligament-alveolar bone interface and scheme of fiber-to-cell contact. **A.** Relationship between the Sharpey's fibers and osteoblasts in the periodontal ligament region of the control samples revealed by electron micrograph. **B.** An enlarged view of the highlighted box in **A.** The osteoblasts located on the surface of the intrinsic alveolar bone contact the collagen fibrils as indicated by red arrows. **C.** Scheme of fiber-to-cell contact. Red spots show tight contact between osteoblasts and Sharpey's fibers. pl: periodontal ligament; ob: osteoblast; ab: alveolar bone. A, x 4000; B, x 6000

alveolar bone model.

Acknowledgements. This study was partially supported by grants from the Ministry of Education, Culture, Sports, Science & Technology and the Japanese Society for the Promotion of Science (to Li M, Amizuka N). National Nature Science Foundation of China (81271965) and Specialized Research Fund for the Doctoral Program of Higher Education (20120131110073) to Li M.

References

Adachi T., Aonuma Y., Taira K., Hojo M. and Kamioka H. (2009). Asymmetric intercellular communication between bone cells: propagation of the calcium signaling. Biochem. Biophys. Res. Commun. 389, 495-500.

Al-Dujaili S.A., Lau E., Al-Dujaili H., Tsang K., Guenther A. and You L. (2011). Apoptotic osteocytes regulate osteoclast precursor recruitment and differentiation in vitro. J. Cell Biochem. 112, 2412-2423.

Burger E.H. and Klein-Nulend J. (1999). Mechanotransduction in bone-role of the lacuno-canalicular network. FASEB J. 13, 101-112.

Cowin S.C. (2002). Mechanosensation and fluid transport in living bone. J. Musculoskelet. Neuronal Interact. 2, 256-260.

Damian C.G., Curtis J.K., Zhang Y., Clare E.Y. and Henry J.D. (2007). Oscillating fluid flow activation of gap junction hemichannels induces ATP release from MLO-Y4 osteocytes. J. Cell. Physiol. 212, 207-214

Doty S.B. (1981). Morphological evidence of gap junction between bone cells. Calcify Tissue Int. 33, 509-512.

Ejiri S. and Ozawa H. (1982). Scanning electron microscopic observations of rat tibia using the HCI-collagenase method. Arch. Histol. 45, 399-404.

Fuller K., Wong B., Fox S., Choi Y. and Chambers T.J. (1998). TRANCE is necessary and sufficient for osteoblast-mediated activation of bone resorption in osteoclasts. J. Exp. Med. 188, 997-1001.

Ishikawa S., Iwasaki K., Komaki M. and Ishikawa I. (2004). Role of ascorbic acid in periodontal ligament cell differentiation. J. Periodontol. 75, 709-716.

Kapur S.P. and Russell T.E. (1978). Sharpey fiber bone development in surgically implanted dog mandible. A scanning electron-microscopic study. Acta. Anat. (Basel) 102, 260-264.

Kufahl R.H. and Saha S. (1989). A theoretical model for stress-generated fluid flow in the canaliculi-lacunae network in bone tissue. J. Biomechanics 23, 171-180.

Kuroiwa M., Chihara K. and Higashi S. (1994). Electron microscopic studies on Sharpey's fibers in the alveolar bone of rat molars. Kaibogaku Zasshi 69, 776-782.

Li M., Amizuka N., Oda K., Tokunaga K., Ito T., Takeuchi K., Takagi R. and Maeda T. (2004). Histochemical evidence of the initial chondrogenesis and osteogenesis in the periosteum of a rib fractured model: implications of osteocyte involvement in periosteal chondrogenesis. Microsc. Res. Tech. 64, 330-342.

Marotti G., Ferretti M., Muglia M.A., Palumbo C. and Palazzini S. (1992). Aquantitative evaluation of osteoblast-osteocyte relationships on growing endosteal surface of rabbit tibiae. Bone 13, 363-368.

Martinez R.H. and Johnson R.B. (1987). Effects of orthodontic forces on the morphology and diameter of Sharpey fibers of the alveolar bone of the rat. Anat. Rec. 219, 10-20.

Masuki H., Li M., Hasegawa T., Suzuki R., Ying G., Liu Z., Oda K., Yamamoto T., Kawanami M. and Amizuka N. (2010). Immunolocalization of DMP1 and sclerostin in the epiphyseal trabecule and diaphyseal cortical bone of osteoprotegerin deficient mice. Biomed. Res. 31, 307-318.

Mimori K., Komaki M., Iwasaki K. and Ishikawa I. (2007). Extracellular signal-regulated kinase 1/2 is involved in ascorbic acid-induced osteoblastic differentiation in periodontal ligament cells. J. Periodontol. 78, 328-334.

Nakashima T.,, Hayashi M., Fukunaga T., Kurata K., Oh-hora M., Feng J.Q., Bonewald L.F., Kodama T., Wutz A, Wagner E.F., Penninger J.M. and Takayanagi H. (2011). Evidence for osteocyte regulation of bone homeostasis through RANKL expression. Nat Med. 17, 1231-1234.

Oda K., Amaya Y., Fukushi-Irie M., Kinameri Y., Ohsuye K., Kubota I., Fujimura S. and Kobayashi J. (1999). A general method for rapid purification of soluble versions of glycosylphosphatidylinositol-anchored proteins expressed in insect cells: an application for human tissue-nonspecific alkaline phosphatase. J. Biochem. (Tokyo) 126, 694-699.

Ott S.M. (2005). Sclerostin and Wnt signaling--the pathway to bone strength. J. Clin. Endocrinol. Metab. 90, 6741-6743.

Palumbo C., Palazzini S. and Marotti G. (1990). Morphological study of intercellular junctions during osteocyte differentiation. Bone 11, 401-406.

Pavlin D., Dove S.B., Zadro R. and Gluhak-Heinrich J. (2000). Mechanical loading stimulates differentiation of periodontal osteoblasts in a mouse osteoinduction model: effect on type?collagen and alkaline phosphatase genes. Calcif. Tissue Int. 67, 163-172.

Pavlin D., Zadro R. and Gluhak-Heinrich J. (2001). Temporal pattern of stimulation of osteoblast-associated genes during mechanically-induced osteogenesis in vivo: early responses of osteocalcin and type 1 collagen. Connect. Tissue Res. 42, 135-148.

Poole K.E., van Bezooijen R.L., Loveridge N., Hamersma H., Papapoulos S.E., Lowik C.W. and Reeve J. (2005). Sclerostin is a delayed secreted product of osteocytes that inhibits bone formation. FASEB J. 19, 1842-1844.

Saito M., Iwawaki T., Taya C., Yonekawa H., Noda M., Inui Y., Mekada E., Kimata Y., Tsuru A. and Kohno K. (2001). Diphtheria toxin receptor-mediated conditional and targeted cell ablation in transgenic mice. Nature Biotechnol. 19, 746-750.

Semënov M., Tamai K. and He X. (2005). SOST is a ligand for LRP5/LRP6 and a Wnt signaling inhibitor. J. Biol. Chem. 280, 26770-26775.

Shiga M., Kapila Y.L., Zhang Q., Hayami T. and Kapila S. (2003). Ascorbic acid induces collagenase-1 in human periodontal ligament cells but not in MC3T3-E1 osteoblast-like cell: potential association between collagenase expression and changes in alkaline phosphatase phenotype. J. Bone Miner. Res. 18, 67-77.

Takami M., Woo J.T. and Nagai K. (1999). Osteoblastic cells induce fusion and activation of osteoclasts through a mechanism independent of macrophage-colony-stimulating factor production. Cell Tissue Res. 298, 327-334.

Tan S.D., Vries T.J., Kujipers-Jagtman A.M., Semeins C.M., Evert V. and Klein-Nulend J. (2007). Osteocytes subjected to fluid flow inhibit osteoclast formation and bone resorption. Bone 41, 745-751.

Tatsumi S., Ishii K., Amizuka N., Li M., Kobayashi T., Kohno K., Ito M., Takeshita S. and Ikeda K. (2007). Targeted ablation of osteocytes

induces osteoporosis with defective mechanotransduction. Cell Metab. 5, 464-475.

Ubaidus S., Li M., Sultana S., de Freitas P.H., Oda K., Maeda T., Takagi R. and Amizuka N. (2009). FGF23 is mainly synthesized by osteocytes in the regularly distributed osteocytic lacunar canalicular system established after physiological bone remodeling. J. Electron Microsc. (Tokyo). 58, 381-392.

Udagawa N., Takahashi N., Jimi E., Matsuzaki K., Tsurukai T., Itoh K., Nakagawa N., Yasuda H., Goto M., Tsuda E., Higashio K., Gillespie M.T., Martin T.J. and Suda T. (1999). Osteoblasts/stromal cells stimulate osteoclast activation through expression of osteoclast differentiation factor/RANKL but not macrophage colony-stimulating factor: receptor activator of NF-kappa B ligand. Bone 25, 517-523.

Udagawa N., Takahashi N., Yasuda H., Mizuno A., Itoh K., Ueno Y., Shinki T., Gillespie M.T., Martin T.J., Higashio K. and Suda T. (2000). Osteoprotegerin produced by osteoblasts is an important regulator in osteoclast development and function. Endocrinology 141, 3478-3484.

Yajima T., Sakakura Y., Tsuruga E., Hirai T., Ikeda Y., Fujii S. and Shide N. (1999). Collagen-phagocytosing ability of periodontal osteoblasts at the bone surface. Arch. Histol. Cytol. 62, 17-25.

You L., Temiyasathit S., Lee P., Kim C., Tummala P., Yao W., Kingery W., Malone A.M., Kwon R.Y. and Jacobs C.R. (2008). Osteocytes as mechanosensors in the inhibition of bone resorption due to mechanical loading. Bone 42, 172-179.

Accepted September 17, 2012